Journal of Robotics and Control (JRC)
Volume 6, Issue 1, 2025
ISSN: 2715-5072, DOI: 10.18196/jrc.v6i1.23927

Robot-Assisted Upper Limb Rehabilitation Using Imitation Learning

Ismail Ashiru Auta [1*], Ahmed Fares [2], Hiroyasu Iwata [3], Haitham El-Hussieny [4*]
[1, 4] Mechatronics and Robotics Engineering, Egypt-Japan University of Science and Technology, Alexandria, Egypt
[2] Computer Science and Engineering, Egypt-Japan University of Science and Technology, Alexandria, Egypt
[3] Faculty of Science and Engineering, Waseda University, Tokyo, Japan
[2] Electrical Engineering Department, Faculty of Engineering at Shoubra, Benha university, Cairo, Egypt
Email: [1] ismail.auta@ejust.edu.eg, [2] ahmed.fares@ejust.edu.eg,
[3] jubi@waseda.jp, [4] haitham.elhussieny@ejust.edu.eg
*Corresponding Author

***Abstract*—Robotic rehabilitation offers an innovative approach to enhance motor function recovery in patients with upper-limb impairment. However, the primary challenge lies in the development of adaptive and personalized therapies to meet the unique needs of patients. In response to this challenge, this paper presents a Rehabilitation Learning from Demonstration (RLfD) framework, which integrates Dynamic Movement Primitives (DMP) for learning and generalizing movements, and a Model Reference Adaptive Controller (MRAC) for real-time adaptive control. This combination enables a two-link manipulator to accurately replicate and adapt therapist demonstrations specifically designed for upper-limb rehabilitation. Unlike conventional task-specific controllers, which are limited by poor adaptability, minimal feedback, and lack of generalization, our system dynamically adjusts robotic assistance in real time based on the subject's tracking error to optimize therapy outcomes. The objective is to minimize assistance while maximizing patient participation in the rehabilitation process. To facilitate this, the framework employs visual tracking technology to capture therapist demonstrations accurately. Once captured, the DMP component of the framework learns from these movements and generalizes them to new goals, while maintaining the original motion patterns. Our evaluations with a simulated two-link manipulator demonstrated the framework's precise trajectory tracking, robust generalization, and adaptability to disturbances mimicking patient impairments. These tests confirmed the system's ability to follow complex trajectories and adapt to dynamic patient motor functions. The promising results from these evaluations highlight our approach's potential to significantly enhance adaptability and generalization in variable patient conditions, marking a substantial improvement over conventional systems.**

Keywords*— *Dynamic Movement Primitives; Learning by Demonstration; Model Adaptive Control; Personalized Therapy

I. Introduction

Stroke is a global health issue that significantly contributes to mortality and disability, affecting over 101 million people in 2019 [1]–[3]. Over two-thirds of individuals recovering from a stroke endure upper limb motor impairment, with 50% experiencing substantial functional loss six months post-stroke [4]–[7]. Early rehabilitation within the first three months is crucial for motor recovery, making it a key research focus [8]–[14].

Robotic technologies, such as exoskeletons and end-effector robots, significantly enhance outcomes by providing precise and intensive support for repetitive exercises, a benefit confirmed by systematic reviews [15]–[22]. These technologies have emerged to enhance upper limb functionality by offering active, passive, and haptic assistance [23]–[30]. Active assistance helps patients engage in exercises, whereas passive assistance requires no effort from the patient as the robot executes movements. Haptic devices, particularly when combined with virtual reality (VR), enrich rehabilitation by providing sensory feedback [31]–[34].

Problem Statement: Despite these advancements, robotic rehabilitation faces challenges in personalizing treatments according to individual patient needs, which is essential for optimizing recovery and ensuring generalization across diverse patient populations [15], [35]–[43]. The limited availability of therapists and insufficient patient feedback hinders the scalability and effectiveness of these systems. Therefore, the development of rehabilitation robots that integrate patient-specific needs with advanced robotic capabilities is essential for delivering effective and scalable interventions [44]–[51].

To address variability in patient conditions, rehabilitation exercises are often modelled using probabilistic methods, such as Gaussian Mixture Models (GMM) and Gaussian Mixture Regression (GMR), to integrate and analyze behaviors observed in patients [52]–[56]. For instance, GMM has been used to model therapist demonstrations, helping robots provide impedance-based assistance [52], whereas other models, such as a dynamic bicycle cranking system, adjust assistance according to therapist performance [57]. However, these methods face challenges when adapting to variations in patient conditions and external factors. Recent advancements have integrated machine-learning technologies. For example, an Intelligent Assistant for Robotic

Therapy (iART) was developed to replicate therapist behaviors in tasks involving 3D trajectory tracking using Long Short-Term Memory (LSTM) networks [58]. Similarly, a combination of a feedforward neural network and VR-based haptics has been used to model and regenerate therapeutic exercises demonstrated by therapists via teleoperation [59]. However, adapting these systems to accommodate diverse patient conditions continues to present a challenge.

Building on these advances, Dynamic Movement Primitives (DMP) have proven to be highly effective for modelling complex movements [60]–[65]. By modifying the start and goal parameters, DMPs enable robots to adapt seamlessly to new goals, thereby demonstrating strong adaptability and generalization. This is particularly evident in their successful application in tasks such as pick-and-place and water-serving with a Sarcos robot arm [66] and is further demonstrated by a rehabilitation robot that uses a DMP-based motion planner to replicate healthy movement styles with high accuracy in target positioning [67]. Another extension of the DMP application to the Kuka LWR4+ robotic arm showed accurate motion style generalization across tasks, such as pouring and eating, significantly improving trajectory accuracy and DMP database utilization compared with previous methods [68], [69]. However, this system exhibited limitations in executing integrated movements, which were addressed by integrating DMPs with hierarchical deep reinforcement learning, thereby enhancing task efficiency through sequential movement execution on a 6 DOF robot arm [70].

A novel approach further enhances this domain by learning directly from therapist demonstrations in which therapist's movements are observed and replicated by a robot for patient rehabilitation [71]–[74]. This method simplifies the process and does not require deep robotic knowledge from therapists. The integration of DMPs with Learning from Demonstrations (LfD) has proven effective in accurately capturing complex human movements [75]–[80].

In this paper, we propose a Rehabilitation Learning from Demonstration (RLfD) framework that leverages DMP for modeling exercises and MRAC for dynamic assistance adjustment based on real-time patient performance. This innovative approach supports a personalized "assist-as-needed" strategy, addressing the key limitations of conventional methods that require multiple demonstrations, retraining for trajectory changes, and manual controller gain adjustments for each patient. In contrast, our RLfD framework adapts and generalizes across various trajectories and patient needs, without retraining. This system is designed to enable therapists, even those without technical expertise to effectively train robots for personalized rehabilitation. By merging therapists' expertise with robotic precision, the RLfD framework can replicate and adapt exercises in real-time based on patient feedback. We hypothesize that this approach will improve motor function therapy, make advanced robotic therapy more accessible, and potentially redefine standards for integrating technology into patient care, leading to improved outcomes compared with traditional methods. The structure of this paper is outlined as follows. Section II details the RLfD framework, including methodologies for demonstration collection and generation of personalized exercises. Section III demonstrates the application of our framework to a simulated robotic manipulator, in which we evaluate the performance and adaptability of the system. Finally, Section IV concludes the study by summarizing the key findings and outlining future research directions.

II. Rehabilitation Learning from Demonstration

A. System Architecture

The architecture of the proposed Rehabilitation Learning from Demonstration (RLfD) is illustrated in Fig. 1 and comprises of the following components: i) A method for therapist demonstration collection, ii) A Dynamic Movement Primitives (DMP) based system that learns movement primitives from these demonstrations, iii) A module for generating personalized exercises, and iv) An implementation of an adaptation mechanism in feedback control to ensure precise exercise execution. A detailed explanation of each component will be provided in subsequent sections, outlining how the system integrates therapist input into functional exercise routines for patients.

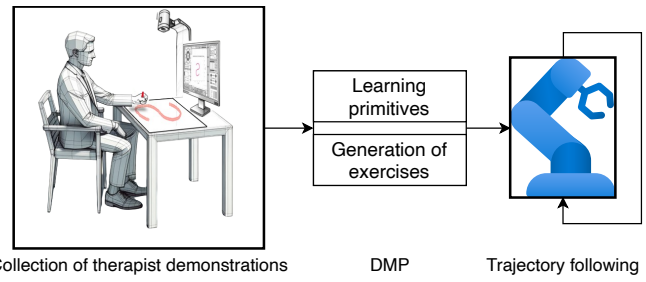

Fig. 1. Block diagram of the proposed RLfD framework, integrating DMP with an adaptive feedback mechanism, enabling a two-link manipulator to replicate and adapt therapist demonstrations for upper limb rehabilitation

B. Collection of Therapist Demonstrations

The process of capturing therapist demonstrations utilized visual tracking to record the therapist's motion in Cartesian coordinates. A visual marker attached to the therapist's wrist was tracked using an RGB camera. The captured pixel coordinates, $\boldsymbol{p} \in \mathbb{R}^2$, are transformed into operational space coordinates, $\boldsymbol{y} \in \mathbb{R}^2$, mapping the camera's observational range, $[C_{\min}, C_{\max}]$, with the robot's operational area, $[R_{\min}, R_{\max}]$:

$$\boldsymbol{y} = \left(\frac{(\boldsymbol{p} - C_{\min}) \times (R_{\max} - R_{\min})}{(C_{\max} - C_{\min})} \right) + R_{\min} \qquad (1)$$

This setup simplifies data collection by converting movements into two-dimensional Cartesian coordinates. Variations in

marker placement, which can affect the accuracy of the tracked coordinates, are smoothed by the DMP system, which will be discussed in the coming sections. The Finite Difference Method is used to calculate velocity $\boldsymbol{v}(t)$ and acceleration $\boldsymbol{a}(t)$, which are necessary inputs for the DMP algorithm:

$$\boldsymbol{v}(t) = \frac{\boldsymbol{y}(t+1) - \boldsymbol{y}(t)}{\Delta t} \tag{2}$$

$$\boldsymbol{a}(t) = \frac{\boldsymbol{v}(t+1) - \boldsymbol{v}(t)}{\Delta t} \tag{3}$$

Following this, the data were normalized for further processing, facilitating the integration of demonstrations into rehabilitation modeling

C. Modeling Rehabilitation Exercises Using Dynamic Movement Primitives

Dynamic Movement Primitives (DMP) are used to represent complex motions via differential equations. Each degree of freedom (DOF) in the system is modeled using second-order differential equations, analogous to the spring-damper mechanism, enhanced by a nonlinear forcing term $\boldsymbol{f}$, which provides the system's unique movement patterns [81]–[85]. The equations governing the system are as follows:

$$\tau\ddot{\boldsymbol{y}} = \alpha\left(\beta\left(\boldsymbol{g} - \boldsymbol{y}\right) - \dot{\boldsymbol{y}}\right) + \boldsymbol{f} \tag{4}$$

Where $\boldsymbol{y}$ and $\dot{\boldsymbol{y}} = \boldsymbol{v}(t)$ represent the position and velocity, respectively, $\boldsymbol{g}$ is the goal position and $\boldsymbol{f}$ is the learned nonlinear forcing term. Parameters τ, α, and β are positive constants that adjust the temporal and spatial characteristics of the motion, affecting the sensitivity of the DMP. τ controls the execution speed, with smaller values increasing sensitivity to rapid adjustments. α influences stability and rigidity, where higher values reduce sensitivity to perturbations. β determines the strength of attraction to the goal, with larger values reducing sensitivity to oscillations. The forcing term $\boldsymbol{f}$, which is essential for capturing unique movement patterns, is modeled as:

$$f\left(x,\ \boldsymbol{g}\right) = \ \frac{\sum_{i=1}^{n}\psi_i\omega_i}{\sum_{i=1}^{n}\psi_i}\ x(\boldsymbol{g} - \boldsymbol{y}_0) \tag{5}$$

Here, ω_i denotes the weights learned from the demonstrations through locally weighted regression, ψ_i are the Gaussian basis functions, and $\boldsymbol{y}_0$ is the initial position. The canonical system controls the temporal dynamics through a phase variable x, which decreases from 1 to 0, thereby ensuring convergence to the goal [86]:

$$\dot{x} = \ -\alpha_x\ x \tag{6}$$

In addition, the Gaussian basis functions are represented as:

$$\psi_i = \exp\left(-h_i\left(x - c_i\right)^2\right) \tag{7}$$

In this equation, h_i and c_i are the width and center of the Gaussians, respectively, which modulate the timing and intensity of each basis function. This allows the DMP to replicate and fine-tune generic motions. The algorithm detailed in Table I and the process illustrated in Fig. 2 demonstrate how the DMP effectively learns and accurately replicates therapist demonstrations.

TABLE I. ALGORITHM FOR DMP ADAPTATION PROCESS

Step	Description
1	Initialize by leveraging the demonstrated trajectories $\boldsymbol{y} = [y_x, y_y]$ to compute the forcing terms $\boldsymbol{f} = [f_1, f_2]$ as defined in Eq. (4).
2	Integrate the canonical system, detailed in Eq. (6), using a fixed α_x to compute the phase variable x.
3	Employ locally weighted regression to adjust the weights ω_i for each basis function in $\boldsymbol{f}$, aiming to minimize the difference between the calculated forces derived from the demonstrated trajectories and the forces from Eq. (5).

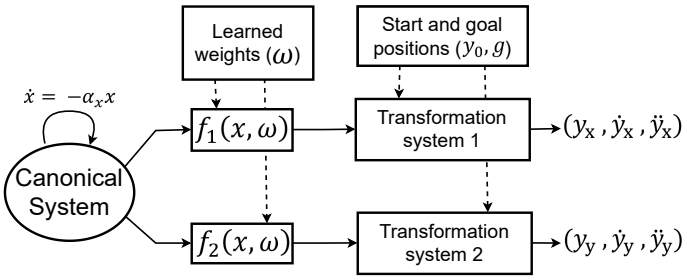

Fig. 2. Schematic of a 2-Dimensional DMP structured into canonical and transformation systems, detailing the process from capturing start ($\boldsymbol{y}_0$) and goal ($\boldsymbol{g}$) positions to computing the learned weights (ω)

D. Personalized Rehabilitation Exercise Generation

DMPs are pivotal in robotic rehabilitation, as they adapt to the changing needs of patients by learning movement patterns from therapist demonstrations. This flexibility allows robots to customize rehabilitation exercises to match the progress of individual patient recovery. For example, as a patient improves, DMPs adjust their exercise difficulty and focus by adjusting their movement trajectories.

These adjustments are achieved by altering key parameters, such as the initial position ($\boldsymbol{y}_0$), goal position ($\boldsymbol{g}$), and temporal scaling (τ) (refer to Eq. (4)) based on predefined criteria such as recovery progress. These criteria determine when and how parameters are adjusted, facilitating the generation of new movement sequences in terms of position ($\boldsymbol{y}$), velocity ($\dot{\boldsymbol{y}}$), and acceleration ($\ddot{\boldsymbol{y}}$) without necessitating model retraining

The effectiveness of motion replication within the RLfD framework was evaluated using Mean Absolute Error (MAE), computed as:

$$MAE = \frac{1}{N}\sum_{t=0}^{N}\left|\boldsymbol{y}_j^d(t) - \boldsymbol{y}_j^r(t)\right| \tag{8}$$

This equation measures the deviation between the demonstrated trajectories ($\boldsymbol{y}_j^d\,(t)$) and the replayed trajectories ($\boldsymbol{y}_j^r\,(t)$) over all time instants ($\boldsymbol{N}$), providing a precise assessment of the trajectory accuracy along each Cartesian axis for $\boldsymbol{j} = 1, 2$.

E. Parameter Optimization Using Particle Swarm Optimization

Particle Swarm Optimization (PSO) is an algorithm motivated by the collective behavior of animals such as birds or fish. Implemented in a multidimensional space, each "particle" represents a potential solution, moving iteratively to explore the search space and improve its position [87]–[91]. The swarm consists of m particles, each with position x_t and velocity v_t. Each particle tracks its optimal position known as p_{best_t} (personal best) and the best position found by any particle in the swarm, g_{best_t} (global best). The particle's velocity and position are updated as follows:

$$\boldsymbol{x}_{t+1} = \boldsymbol{x}_t + \boldsymbol{v}_{t+1} \tag{9}$$

$$\boldsymbol{v}_{t+1} = \boldsymbol{\omega}\boldsymbol{v}_t + c_1 r_1(\boldsymbol{p}_{\text{best}_t} - \boldsymbol{x}_t) + c_2 r_2(\boldsymbol{g}_{\text{best}_t} - \boldsymbol{x}_t) \tag{10}$$

Here, ω balances the exploration and exploitation aspects of the search, whereas c_1 and c_2 are coefficients that guide the particle towards its personal best and global best, respectively. Random variables r_1 and r_2 introduce stochasticity into the updates. Fig. 3 illustrates the process flowchart for the Particle Swarm Optimization (PSO) algorithm.

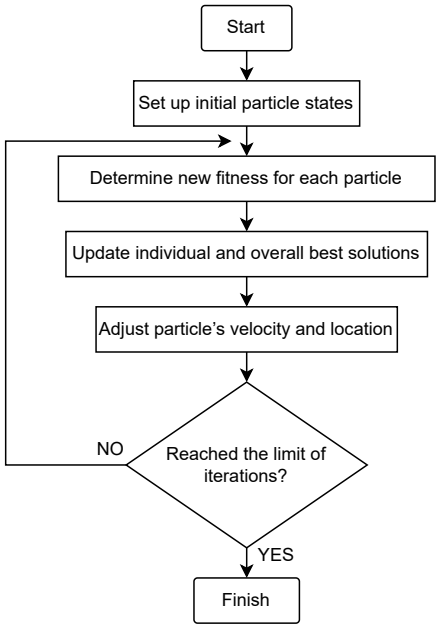

Fig. 3. PSO Algorithm Process Flowchart

PSO is applied to optimize the α and β parameters in the DMP, with the aim of minimizing the trajectory errors defined by the sum of the mean absolute errors in Cartesian coordinates, as follows:

$$\boldsymbol{f}_{\text{val}} = \sum_{i=1}^{n} |x_{\text{r}_i} - x_{\text{d}_i}| + |y_{\text{r}_i} - y_{\text{d}_i}| \tag{11}$$

Where x_{r_i} and y_{r_i} represent the coordinates of the reproduced motion at the i-th iteration, and x_{d_i} and y_{d_i} are the coordinates of the demonstrated motion at the same iteration. The fitness value f_{val} quantifies the cumulative absolute errors between the demonstrated and reproduced motions over the total number of points n in the trajectory. The optimization process using PSO continues until a convergence criterion is met or a predetermined number of iterations are reached.

The decision to use PSO over other optimization techniques, such as Gradient Descent or Genetic Algorithms, is based on its simple implementation and efficiency. Although many methods can minimize errors and optimize parameters, PSO is simple and has the ability to escape local minima, making it well-suited for our application.

F. Model Reference Adaptive Control (MRAC)

The MRAC allows a two-degree-of-freedom robot to precisely track rehabilitation exercises by moving the patient's hand attached to the robot's end effector. This is achieved by employing inverse kinematics to convert these trajectories from task space into joint space using a Jacobian-based controller to calculate essential joint configurations ($\boldsymbol{q}$), ensuring that the robot adheres closely to defined exercise trajectories. It incorporates an adaptive control mechanism that dynamically adjusts the level of assistance provided to the patients based on their performance. This mechanism is depicted in Fig. 4, which highlights how the controller gains ($\boldsymbol{K}$, $\tilde{K}$) are dynamically tuned to optimize the system response.

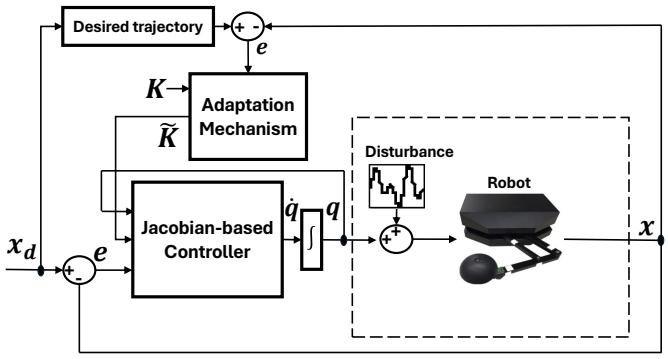

Fig. 4. This block diagram illustrates the control loop involving a Jacobian controller and an adaptation mechanism. It outlines how the system adjusts gains to maintain the desired trajectory ($\boldsymbol{x}_d$) amidst disturbances

*1) **Jacobian-based Controller**:* This control approach depends on several key components: the velocities of the end-effector ($\dot{\boldsymbol{x}}_r$), which describe how quickly the end-effector's

position changes; the velocities of the joints ($\dot{\boldsymbol{q}}$), indicating the rate of change in the robot's joint angles; Central to this relationship is the Jacobian matrix $\boldsymbol{J}(\boldsymbol{q})$, which is determined by the partial derivative of the end-effector's position with respect to joint angles: $\partial \boldsymbol{x}/\partial \boldsymbol{q}$ [92]–[94]. The Jacobian matrix maps the joint velocities into the velocities of the end-effector, as shown in the equation below:

$$\dot{\boldsymbol{x}_r} = \boldsymbol{J}(\boldsymbol{q})\dot{\boldsymbol{q}} \tag{12}$$

The joint velocities are computed by inverting the Jacobian:

$$\dot{\boldsymbol{q}} = \boldsymbol{J}^{-1}(\boldsymbol{q})\dot{\boldsymbol{x}_r} \tag{13}$$

Joint states $\boldsymbol{q}$ are updated by integrating these velocities for accurate tracking of the desired trajectory ($\dot{\boldsymbol{x}}_d$), with error compensation ($\mathbf{e} = \boldsymbol{x}_d - \boldsymbol{x}_r$). In the case of our robot, the inversion of the square Jacobian matrix is simplified, ensuring precise trajectory tracking and preventing numerical drift. Modified joint velocities are defined as:

$$\dot{\boldsymbol{q}} = \boldsymbol{J}_A^{-1}(\boldsymbol{q})\left(\dot{\boldsymbol{x}}_d + \boldsymbol{K}\mathbf{e}\right) \tag{14}$$

Where $\boldsymbol{K} \in \mathbb{R}^{2\times 2}$, a positive definite matrix, enhances system convergence and stability. Alternatively, using the transpose of the Jacobian matrix:

$$\dot{\boldsymbol{q}} = \boldsymbol{J}_A^{T}(\boldsymbol{q})\boldsymbol{K}\mathbf{e} \tag{15}$$

Minimizes tracking errors and improves responsiveness to dynamic changes, thereby refining the system's performance [95].

*2) **Adaptive Assistance Mechanism**:* To enhance patient engagement, the controller gains $\boldsymbol{K}$ are dynamically adjusted based on real-time performance. The adaptive mechanism employs a strategy that includes error thresholds and a delay-based stabilization feature to moderate gain adjustments. The adaptation algorithm outlined below operates independently for each component (x and y) of the end-effector's error $\mathbf{e}$.

The specific adaptations are given by:

$$\tilde{\boldsymbol{K}}_i = \begin{cases} \boldsymbol{K}_i \cdot (1 + |\boldsymbol{e}_i| \cdot r) & \text{if } |\boldsymbol{e}_i| > \text{threshold}_i \\ \boldsymbol{K}_i & \text{if } |\boldsymbol{e}_i| < \text{threshold}_i \text{ and} \\ & \text{delay counter} > \text{delay threshold} \end{cases}$$

for $i \in \{x, y\}$, where K_i is the gain for direction i, e_i is the error in direction i, and r is the adaptation rate. This structured approach ensures that assistance levels are both responsive and moderated, thus optimizing the support provided based on the patient's immediate needs and performance. Specifically, this adaptation mechanism responds to different disturbances by increasing the gains when errors exceed a defined threshold, enhancing the robotic intervention to counter significant deviations and aiding in rapid correction. For smaller errors or when errors are within normal bounds, a delay-based stabilization feature moderates the gain adjustments, preventing over correction and ensuring stability.

Algorithm 1: Adaptation Algorithm for Robotic Assistance

```
Result: Adjust robotic gains based on error
initialization;
while System Running do
    measure error |e_i|;
    if |e_i| > threshold then
        adjust gains K̃_i = K_i · (1 + |e_i| · r);
    else
        check delay counter;
        if delay counter > delay threshold then
            reset gains K̃_i = K_i;
        end
    end
end
```

III. Simulation Results and Discussion

The RLfD framework, utilizing the parameters outlined in Table II, has been implemented to facilitate the effective learning and adaptation of therapeutic movements by a two-link robot for upper limb rehabilitation, as validated through both real and simulated environments.

TABLE II. Parameters for the RLfD Framework

Parameters	Description	Value
n	Number of basis functions	60
α	DMP gain term	9.8
β	DMP gain term	37.5
α_x	Canonical decay rate	0.8
τ	Temporal Scaling Factor	1
r	Adaptation Rate	50
K	Controller gain (K)	[1 1]
l_i	Link lengths	[50, 50] cm

Initially, we employed visual tracking with an RGB camera to capture rehabilitation motions, as outlined in the RLfD framework. We recorded two demonstrations (refer to Fig. 5), where human subjects moved their labelled wrists within the camera's range to generate therapeutic motions. These motions were then converted from pixel to Cartesian coordinates via equation 1, and parameters specified in Table II. We focused on appropriate movements for a two-link manipulator, such as the exercises depicted in Fig. 5. These exercises requires tracing a distinct pattern on a horizontal plane through the navigation of alternating and intersecting curves to enhance motor control and coordination.

Once the desired motion is captured in Cartesian coordinates, it serves as the foundational data that is then input into the DMP to compute the target forcing term f. This process was specifically aimed at learning, replicating, and generalizing the

recorded motion. To refine this learning process, the DMP system employs locally weighted regression and evenly distributed basis functions (see Fig. 6) to effectively determine the necessary weights for each degree of freedom (DOF), which are essential for accurate replication. Furthermore, Particle Swarm Optimization (PSO) was utilized to fine-tune the parameters α and β of the DMP system.

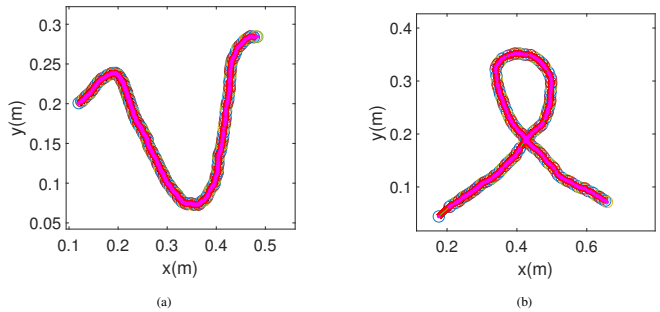

Fig. 5. Demonstrations collected during training: showcasing two distinct exercises performed by the therapist

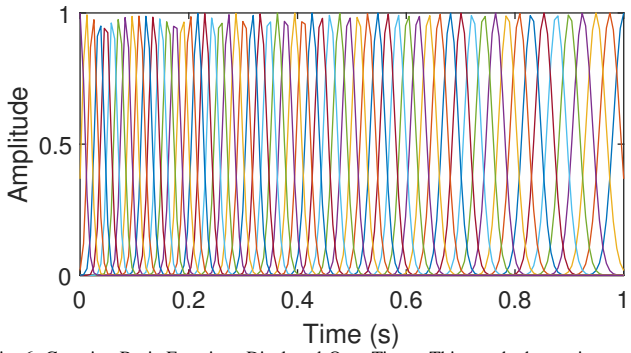

Fig. 6. Gaussian Basis Functions Displayed Over Time - This graph shows sixty equally spaced Gaussian distributions, each representing a unique basis function, highlighting the variation in amplitude and spacing throughout the observed period

The PSO algorithm, configured with a swarm size of 10 particles and limited to 30 iterations, converged with an average computation time of 33.5 seconds and an objective function value of 0.0024. The search space was defined within bounds for α and β set between [0, 0] and [50, 50], respectively, allowing for a broad but constrained exploration of parameter values. Parameters α and β are non-negative because they represent coefficients that scale damping and stiffness forces in the DMP equations. Setting a lower bound of zero ensures that the system can start without any inherent motion or force. On the other hand, an upper limit of 50 represents a practical threshold beyond which the system becomes unstable. This setup was chosen to balance exploration and exploitation efficiently within the defined parameter space.

The optimal parameters achieved through the PSO are $\alpha = 9.8$ and $\beta = 37.5$. This optimization improves the model's adjustment to the movement's dynamic properties, thereby enhancing the precision of trajectory reproduction. The progression of the PSO optimization is depicted in Fig. 7, which shows the **Trajectory Error Function**. This function represents the best value achieved, indicating the lowest trajectory error among all particles, and its decrease over time illustrates the effective tuning of the parameters.

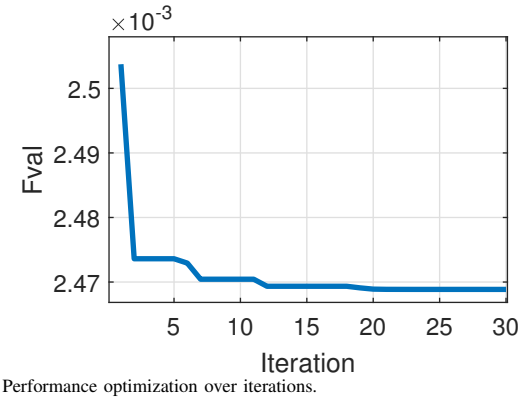

Fig. 7. Performance optimization over iterations.

Fig 8 demonstrates how the DMP system accurately replicated this trajectory with negligible deviation, yielding a total positional error of approximately 0.25 cm across both the x and y directions, as shown in Fig. 9. The integration of PSO in tuning the DMP parameters clearly contributed to the high precision of trajectory reproduction observed during these experiments.

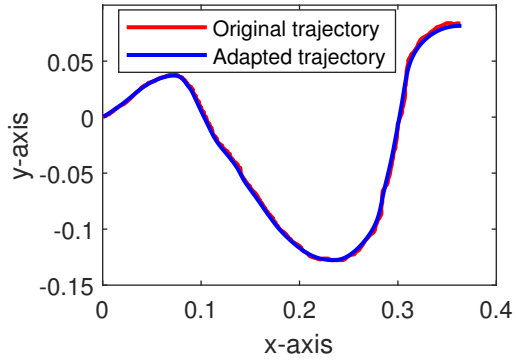

Fig. 8. This graph shows the demonstrated trajectory and the reproduced trajectory generated through the DMP.

The Mean Absolute Error (MAE) serves as the key metric for evaluating the accuracy of the system's ability to replicate the therapist's original motion. The MAE values measure the average deviation between the reproduced trajectory and the therapist's demonstrated motion across the x- and y-axes in the Cartesian coordinates. Specifically, the MAE values for the x- and y-positions were 0.09 cm and 0.16 cm, respectively. These lower MAE values indicated a higher degree of accuracy, signifying that the system accurately mimicked the therapist's movement style. This effectiveness in accurately reproducing

therapeutic exercises demonstrates the potential of this system for precise motion reproduction.

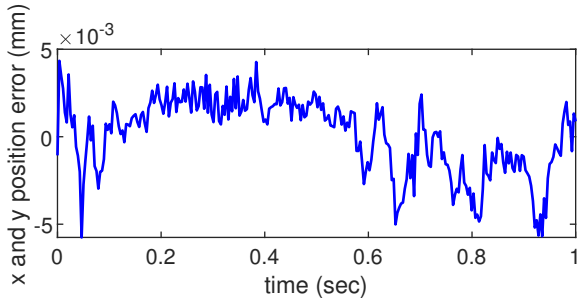

Fig. 9. Variations in x and y positional errors over time during trajectory reproduction

The adaptability of the DMP to new goals was evaluated by modifying the goal point of the demonstrated trajectory while retaining the original starting conditions and the previously learned weights, as shown in Fig. 10. The DMP effectively adjusted the motion to meet the new goal without altering the inherent pattern of the original trajectory. This capability is particularly advantageous for repetitive therapeutic exercises which require modifications to cater for different recovery stages or patient needs with varying goals, as it removes the need to repeatedly retrain the robot for each specific target.

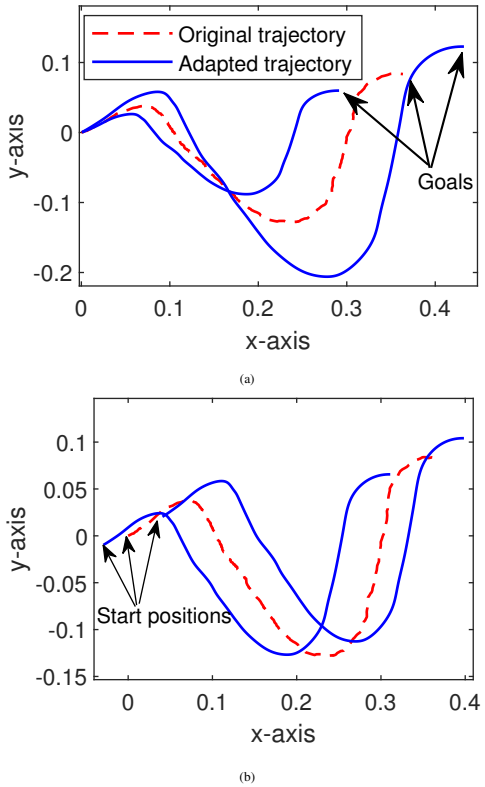

Fig. 10. Demonstrated Trajectory Adaptations. Figure (a) Original trajectory and adaptation to various goals Figure (b) Original and adapted trajectories, each with different starting points and goals

In comparing the adaptability and reproduction capabilities of the DMP with other models, such as those used in Martinez et al. [96], Najafi et al. [97], and Lauretti et al. [68], DMPs show several advantages. DMPs demonstrated superior reproduction abilities, achieving minimal deviation (MAE: 0.09 cm, 0.16 cm) compared to the errors observed in Martinez et al.'s GMM/GMR-based framework (2.9926 cm) and Lauretti et al.'s NDE range (2.4 cm to 3.4 cm). Lastly, DMPs excelled in **generalizability**, easily adapting to new goals by adjusting parameters, unlike models requiring task-specific tuning, as in Najafi et al. (2017) and Pareek et al. [58].

A. Robot Design and Simulation

This study's simulation process involves designing a two-link manipulator in SolidWorks and subsequently importing it into MATLAB's Simscape for kinematic simulations. The simulation was configured with a fixed sampling time of 0.1 seconds, running for a total duration of 39.91 seconds. Performance of the RLfD framework in tracking the recorded trajectory was assessed by configuring the robot to follow trajectories formulated by the DMP, which were then incorporated into the MRAC. This conversion of task-space trajectories into joint-space commands enabled precise robotic execution of the movements, illustrating a smooth transition of task-space modeling into practical robotic actions. It was initially assumed that the patient would need assistance to complete the movement tasks.

Fig. 11 illustrates how the robot tracked the demonstrated trajectory, showing the precision with which it closely adhered to the desired path. This level of tracking highlights the effectiveness of the dynamically adjusted controller gains $\boldsymbol{K}$, which are modulated in real time based on the performance metrics. Specifically, the adaptation mechanism employs error thresholds and a delay-based stabilization feature to moderate gain adjustments.

During the simulation, when the error $\mathbf{e}$ in any direction exceeded predefined thresholds (1.5cm for both directions), robotic assistance was triggered, and the corresponding gains were proportionally adjusted according to the error magnitude at a predefined rate $\boldsymbol{r}$. This intensified the support in response to greater deviations, ensuring that the robot maintained close conformity to the desired trajectory. Conversely, if the error falls below these thresholds, assistance is deactivated, allowing the patient to deviate within these predefined limits, thereby promoting a more interactive rehabilitation process. Moreover, a delay-counter mechanism ensures that overcompensation is avoided by resetting the gains to their baseline when the performance stabilizes. The simulation results validated the MRAC's ability both to provide tailored robotic assistance based on real-time error evaluation and to facilitate precise control over the robot's movements, allowing for complex rehabilitation tasks within a 2D environment.

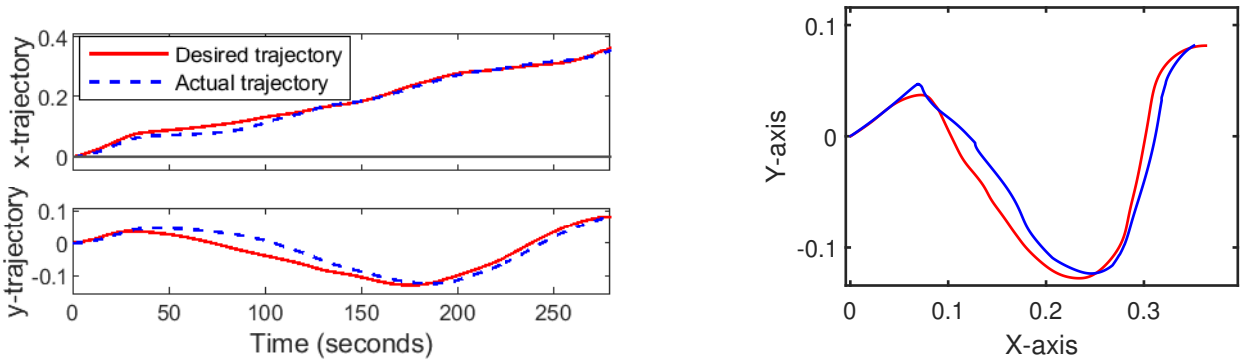

(a) (b)

Fig. 11. Comparative Analysis of Trajectory Tracking: (a) illustrates the robot's performance over time, tracking both the desired and actual trajectories along the x and y axes. (b) Depicts the robot's path in a 2D plane, contrasting the desired trajectory with the actual movement, and highlighting the precision within the allowable error threshold

B. Assessing Robustness Against Impairments

The resilience and trajectory accuracy of the MRAC were rigorously tested by introducing impulse disturbances to the position of the end effector during motion, as illustrated shown in Fig. 12. These disturbances are designed to simulate motor impairments commonly encountered by patients during therapy, providing a test of the system beyond standard conditions.

Before the disturbances were added, as shown in Fig. 11, the MRAC demonstrated high fidelity in tracking the demonstrated path and dynamically adjusting gains based on real-time error evaluation. This initial performance sets a high benchmark for the system resilience.

Upon the addition of disturbances, Fig. 13 captures the adaptable gain's response to the patient's trajectory deviations in both directions. Despite these disturbances, the MRAC demonstrated remarkable adaptability, swiftly adjusting the controller parameters when the error was above the allowable threshold to correct deviations and was closely aligned with the desired trajectory. The comprehensive results from these tests, detailing the most effective settings for the gain values and adaptation rate parameters, are listed in Table II. In summary, our work's key contributions lie in integrating DMP and MRAC within the RLfD framework, enhancing personalization and adaptability in therapeutic exercises. Simulated tests with a two-link robot demonstrated adaptability to impulse disturbances mimicking motor impairments and precise control. These results show significant improvements over conventional rehabilitation methods, setting a foundation for future research with physical robots.

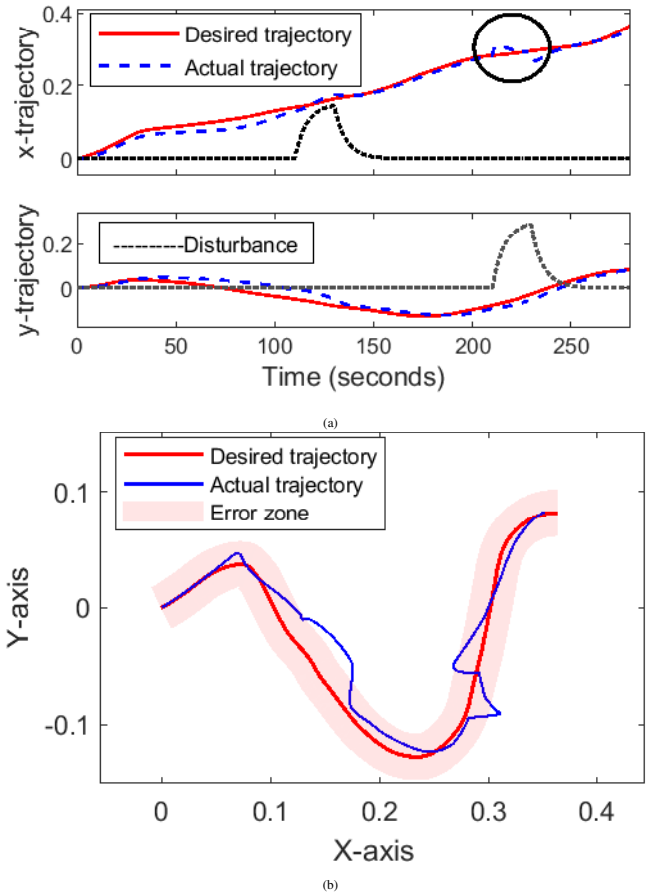

(a) (b)

Fig. 12. Trajectory Tracking with Added Disturbance: (a) time-based analysis of the x and y axes, highlighting deviations and the system's compensatory adjustments in response to disturbances. (b) Illustration of the robot's path in a 2D plane, demonstrating the impact of disturbances on tracking accuracy

IV. Conclusion and Future Works

This paper introduces an innovative approach to robotic-assisted therapy for the upper limb, leveraging Rehabilitation Learning from Demonstration (RLfD) framework to model therapeutic exercises based on therapist demonstrations. By integrating Dynamic Movement Primitives (DMP) to model intricate motor functions and employing the Model Reference Adaptive Controller (MRAC) to facilitate adaptive learning capabilities, the framework significantly enhances both the personalization and adaptability of therapeutic exercises.

The DMP system demonstrated remarkable precision in reproducing recorded trajectories, with Mean Absolute Error (MAE) values of 0.09 cm and 0.16 cm across the x- and y-axes, respectively. Additionally, the system showed exceptional resilience and adaptability, effectively handling disturbances by swiftly adjusting the controller parameters to correct deviations and maintain the desired trajectory. This adaptability was particularly notable during real-time adjustments, which were based on predefined error thresholds, ensuring that assistance was provided dynamically to promote patient engagement and autonomy in therapy.

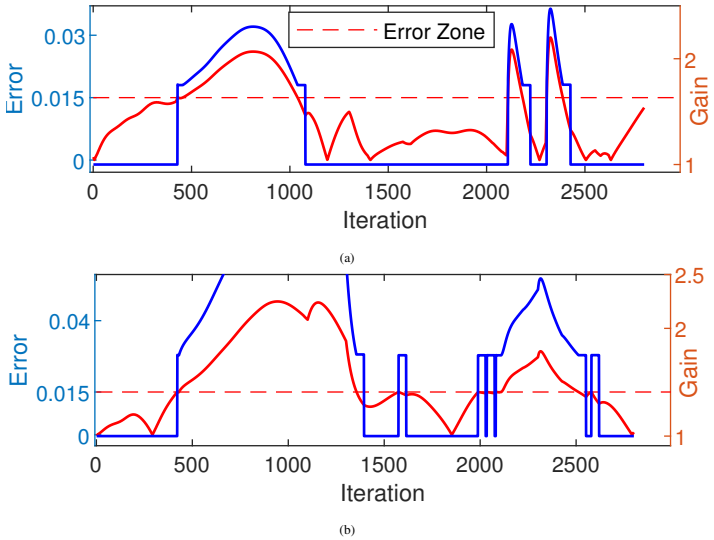

Fig. 13. The plots display the controller gain and error trajectories for both x and y directions, with the predefined error zone indicated by the dashed line. They highlighted the dynamic adjustments of gains in response to fluctuating errors across different axes, showcasing the controller's adaptability.

The capabilities of this system were rigorously tested in a 2D simulation environment, where a two-link robot demonstrated its ability to perform essential upper limb rehabilitation movements. To accurately simulate the variability in patient performance, impulse disturbances mimicking motor impairments were introduced at the position of the end-effector. This rigorous testing, which incorporated error thresholds and delay-based stabilization features into the MRAC, confirmed the robustness and adaptability of the system.

These tests confirmed the system's potential for real-time, personalized rehabilitation. However, while simulation results are promising, practical implementation of this technology requires further validation. Future research should prioritize empirical testing with physical robots to assess effectiveness and safety in real-world scenarios. Advancing to 3D simulations and testing environments is crucial to enhance applicability, ensure robustness, and prepare for complex rehabilitation scenarios.

REFERENCES

[1] A. Demeco, L. Zola, A. Frizziero, C. Martini, A. Palumbo, R. Foresti, G. Buccino, and C. Costantino, "Immersive virtual reality in post-stroke rehabilitation: A systematic review," *Sensors*, vol. 23, no. 3, 2023, doi: 10.3390/s23031712.

[2] N. Marotta, A. Ammendolia, C. Marinaro, A. Demeco, L. Moggio, and C. Costantino, "International classification of functioning, disability and health (icf) and correlation between disability and finance assets in chronic stroke patients," *Acta Bio Medica: Atenei Parmensis*, vol. 91, no. 3, 2020, doi: 10.23750/abm.v91i3.8968.

[3] G. Collaborators and Feigin, "Global, regional, and national burden of stroke and its risk factors, 1990–2019: a systematic analysis for the global burden of disease study 2019," *The Lancet Neurology*, vol. 20, no. 10, pp. 795–820, 2021, doi: 10.1016/S1474-4422(21)00252-0.

[4] A. Demeco, R. Foresti, A. Frizziero, N. Daracchi, F. Renzi, M. Rovellini, A. Salerno, C. Martini, L. Pelizzari, and C. Costantino, "The upper limb orthosis in the rehabilitation of stroke patients: The role of 3d printing," *Bioengineering*, vol. 10, no. 11, 2023, doi: 10.3390/bioengineering10111256.

[5] C. M. Stinear, C. E. Lang, S. Zeiler, and W. D. Byblow, "Advances and challenges in stroke rehabilitation," *The Lancet Neurology*, vol. 19, no. 4, pp. 348–360, 2020, doi: 10.1016/S1474-4422(19)30415-6.

[6] K. S. Hayward, S. F. Kramer, E. J. Dalton, G. R. Hughes, A. Brodtmann, L. Churilov, G. Cloud, D. Corbett, L. Jolliffe, T. Kaffenberger, V. Rethnam, V. Thijs, N. Ward, N. Lannin, and J. Bernhardt, "Timing and dose of upper limb motor intervention after stroke: A systematic review," *Stroke*, vol. 52, no. 11, pp. 3706–3717, 2021, doi: 10.1161/STROKEAHA.121.034348.

[7] R. Bertani, C. Melegari, M. C. De Cola, A. Bramanti, P. Bramanti, and R. S. Calabrò, "Effects of robot-assisted upper limb rehabilitation in stroke patients: a systematic review with meta-analysis," *Neurological Sciences*, vol. 38, pp. 1561–1569, 2017, doi: 10.1007/s10072-017-2995-5.

[8] L. A. Simpson, K. S. Hayward, M. McPeake, T. S. Field, and J. J. Eng, "Challenges of estimating accurate prevalence of arm weakness early after stroke," *Neurorehabilitation and Neural Repair*, vol. 35, no. 10, pp. 871–879, 2021, doi: 10.1177/15459683211028240.

[9] A. G. Doğan, "The effect of occupational therapy on upper extremity function and activities of daily living in hemiplegic patients," *Journal of Medicine and Palliative Care*, vol. 4, pp. 350–354, 2023, doi: 10.47582/jompac.1327960.

[10] B. Zhang, K.-P. Wong, and J. Qin, "Effects of virtual reality on the limb motor function, balance, gait, and daily function of patients with stroke: Systematic review," *Medicina*, vol. 59, no. 4, 2023.

[11] J. Huang, J.-R. Ji, C. Liang, Y.-Z. Zhang, H.-C. Sun, Y.-H. Yan, and X.-B. Xing, "Effects of physical therapy-based rehabilitation on recovery of upper limb motor function after stroke in adults: a systematic review and meta-analysis of randomized controlled trials," *Annals of Palliative Medicine*, vol. 11, no. 2, pp. 521–531, 2022, doi: 10.21037/apm-21-3710.

[12] "Upper limb robot-assisted rehabilitation versus physical therapy on subacute stroke patients: A follow-up study," *Journal of Bodywork and Movement Therapies*, vol. 24, no. 1, pp. 194–198, 2020, doi: 10.1016/J.JBMT.2019.03.016.

[13] M. Coscia, M. J. Wessel, U. Chaudary, J. d. R. Millán, S. Micera, A. Guggisberg, P. Vuadens, J. Donoghue, N. Birbaumer, and F. C. Hummel, "Neurotechnology-aided interventions for upper limb motor rehabilitation in severe chronic stroke," *Brain*, vol. 142, no. 8, pp. 2182–2197, 2019, doi: 10.1093/brain/awz181.

[14] J. Bernhardt *et al.*, D. Corbett, and S. C. Cramer, "A stroke recovery trial development framework: Consensus-based core recommendations from the second stroke recovery and rehabilitation roundtable," *International Journal of Stroke*, vol. 14, no. 8, pp. 792–802, 2019, doi: 10.1177/1747493019879657.

[15] H. R. E. Reem M. Al-Whaibi, Maher S. Al-Jadid and W. M. Badawy, "Effectiveness of virtual reality-based rehabilitation versus conventional therapy on upper limb motor function of chronic stroke patients: a systematic review and meta-analysis of randomized controlled trials," *Physiotherapy Theory and Practice*, vol. 38, no. 13, pp. 2402–2416, 2022, doi: 10.1080/09593985.2021.1941458.

[16] A. N. Malik, H. Tariq, A. Afridi, and F. A. Rathore, "Technological advancements in stroke rehabilitation," *Journal of Pakistan Medical Association*, vol. 72, no. 8, pp. 1672–1674, 2022, doi: 10.47391/JPMA.22-90.

[17] M. Kyrarini, F. Lygerakis, A. Rajavenkatanarayanan, C. Sevastopoulos, H. R. Nambiappan, K. K. Chaitanya, A. R. Babu, J. Mathew, and F. Makedon, "A survey of robots in healthcare," *Technologies*, vol. 9, no. 1, 2021, doi: 10.3390/TECHNOLOGIES9010008.

[18] M. Germanotta, L. Cortellini, S. Insalaco, and I. Aprile, "Effects of upper limb robot-assisted rehabilitation compared with conventional therapy in patients with stroke: Preliminary results on a daily task assessed using motion analysis," *Sensors*, vol. 23, no. 6, 2023, doi: https://doi.org/10.3390/s23063089.

[19] S. Giovannini, C. Iacovelli, F. Brau, C. Loreti, A. Fusco, P. Caliandro, L. Biscotti, L. Padua, R. Bernabei, and L. Castelli, "Robotic-assisted rehabilitation for balance and gait in stroke patients (roar-s): study protocol for a preliminary randomized controlled trial," *Trials*, vol. 23, 2022, doi: 10.1186/s13063-022-06812-w.

[20] S. B. Reis, W. M. Bernardo, C. A. Oshiro, H. I. Krebs, and A. B. Conforto, "Effects of robotic therapy associated with noninvasive brain stimulation on upper-limb rehabilitation after stroke: Systematic review and meta-analysis of randomized clinical trials," *Neurorehabilitation and Neural Repair*, vol. 35, no. 3, pp. 256–266, 2021, doi: 10.1177/1545968321989353.

[21] I. Aprile, G. Guardati, V. Cipollini, D. Papadopoulou, A. Mastrorosa, L. Castelli, S. Monteleone, A. Redolfi, S. Galeri, and M. Germanotta, "Robotic rehabilitation: An opportunity to improve cognitive functions in subjects with stroke. an explorative study," *Frontiers in Neurology*, vol. 11, 2020, doi: 10.1177/1545968321989353.

[22] R. Iandolo, F. Marini, M. Semprini, M. Laffranchi, M. Mugnosso, A. Cherif, L. De Michieli, M. Chiappalone, and J. Zenzeri, "Perspectives and challenges in robotic neurorehabilitation," *Applied Sciences*, vol. 9, no. 15, 2019, doi: 10.3390/APP9153183.

[23] P. Maciejasz, J. Eschweiler, K. Gerlach-Hahn, A. Jansen-Troy, and S. Leonhardt, "A survey on robotic devices for upper limb rehabilitation," *Journal of NeuroEngineering and Rehabilitation*, vol. 11, no. 3, 2014, doi: 10.1186/1743-0003-11-3.

[24] J. Narayan, B. Kalita, and S. K. Dwivedy, "Development of robot-based upper limb devices for rehabilitation purposes: a systematic review," *Augmented Human Research*, vol. 6, no. 4, 2021, doi: 10.1007/s41133-020-00043-x.

[25] S. Bhujel and S. Hasan, "A comparative study of end-effector and exoskeleton type rehabilitation robots in human upper extremity rehabilitation," *Human-Intelligent Systems Integration*, vol. 5, pp. 11–42, 2023, doi: 10.1007/s42454-023-00048-y.

[26] Y. Shen, P. W. Ferguson, and J. Rosen, "Upper limb exoskeleton systems: Overview," *Journal of Robotics Research*, vol. 45, no. 2, pp. 1–22, 2020, doi: 10.1007/s42454-023-00048-y.

[27] J. F. Mullen, J. Mosier, S. Chakrabarti, A. Chen, T. White, and D. P. Losey, "Communicating inferred goals with passive augmented reality and active haptic feedback," *IEEE Robotics and Automation Letters*, vol. 6, no. 4, pp. 8522–8529, 2021, doi: 10.1109/LRA.2021.3111055.

[28] J. Zheng, P. Shi, M. Fan, S. Liang, S. Li, and H. Yu, "Effects of passive and active training modes of upper-limb rehabilitation robot on cortical activation: a functional near-infrared spectroscopy study," *NeuroReport*, vol. 32, no. 6, pp. 479–488, 2021, doi: 10.1097/WNR.0000000000001615.

[29] Z. Zhao, J. Xiao, H. Jia, H. Zhang, and L. Hao, "Prescribed performance control for the upper-limb exoskeleton system in passive rehabilitation training tasks," *Applied Sciences*, vol. 11, no. 21, 2021, doi: 10.3390/app112110174.

[30] A. Nasr, C. R. Dickerson, and J. McPhee, "Experimental study of fully passive, fully active, and active–passive upper-limb exoskeleton efficiency: An assessment of lifting tasks," *Sensors*, vol. 24, no. 1, 2024, doi: 10.3390/s24010063.

[31] N. Norouzi-Gheidari, P. S. Archambault, K. Monte-Silva, D. Kairy, H. Sveistrup, M. Trivino, M. F. Levin, and M.-H. Milot, "Feasibility and preliminary efficacy of a combined virtual reality, robotics and electrical stimulation intervention in upper extremity stroke rehabilitation," *Journal of NeuroEngineering and Rehabilitation*, vol. 18, no. 1, 2021, doi: 10.1186/s12984-021-00851-1.

[32] F. Zanatta, A. Giardini, A. Pierobon, M. D'Addario, and P. Steca, "A systematic review on the usability of robotic and virtual reality devices in neuromotor rehabilitation: patients' and healthcare professionals' perspective," *BMC Health Services Research*, vol. 22, no. 1, 2022, doi: 10.1186/s12913-022-07821-w.

[33] W. E. Clark, M. Sivan, and R. J. O'Connor, "Evaluating the use of robotic and virtual reality rehabilitation technologies to improve function in stroke survivors: A narrative review," *Journal of Rehabilitation and Assistive Technologies Engineering*, vol. 6, 2019, doi: 10.1177/2055668319863557.

[34] A. Chillura *et al*., "Advances in the rehabilitation of intensive care unit acquired weakness: A case report on the promising use of robotics and virtual reality coupled to physiotherapy," *Medicine*, vol. 99, no. 28, 2020, doi: 10.1097/MD.0000000000020939.

[35] F. Yakub, A. Z. Md. Khudzari, and Y. Mori, "Recent trends for practical rehabilitation robotics, current challenges and the future," *International Journal of Rehabilitation Research*, vol. 37, no. 1, pp. 9–21, 2014, doi: 10.1097/MRR.0000000000000035.

[36] T. Takebayashi, K. Takahashi, Y. Okita, H. Kubo, K. Hachisuka, and K. Domen, "Impact of the robotic-assistance level on upper extremity function in stroke patients receiving adjunct robotic rehabilitation: sub-analysis of a randomized clinical trial," *Journal of NeuroEngineering and Rehabilitation*, vol. 19, no. 1, 2022, doi: 10.1186/s12984-022-00986-9.

[37] F. Yuan, E. Klavon, Z. Liu, R. P. Lopez, and X. Zhao, "A systematic review of robotic rehabilitation for cognitive training," *Frontiers in Robotics and AI*, vol. 8, 2021, doi: 10.3389/frobt.2021.605715.

[38] K. Nizamis, A. Athanasiou, S. Almpani, C. Dimitrousis, and A. Astaras, "Converging robotic technologies in targeted neural rehabilitation: A review of emerging solutions and challenges," *Sensors*, vol. 21, no. 6, 2021, doi: 10.3390/s21062084.

[39] C. Giang, E. Pirondini, N. Kinany, C. Pierella, A. Panarese, M. Coscia, J. Miehlbradt, C. Magnin, P. Nicolo, A. Guggisberg, and S. Micera, "Motor improvement estimation and task adaptation for personalized robot-aided therapy: a feasibility study," *BioMedical Engineering OnLine*, vol. 19, no. 1, 2020, doi: 10.1186/s12938-020-00779-y.

[40] P. V. V. Shahid Hussain, Prashant K. Jamwal and N. A. T. Brown, "Robot assisted ankle neuro-rehabilitation: State of the art and future challenges," *Expert Review of Neurotherapeutics*, vol. 21, no. 1, pp. 111–121, 2020, doi: 10.3390/app112110174.

[41] J. Bessler, G. B. Prange-Lasonder, L. Schaake, J. F. Saenz, C. Bidard, I. Fassi, M. Valori, A. B. Lassen, and J. H. Buurke, "Safety assessment of rehabilitation robots: A review identifying safety skills and current knowledge gaps," *Frontiers in Robotics and AI*, vol. 8, 2021, doi: 10.3389/frobt.2021.602878.

[42] A. Gupta, A. Singh, V. Verma, A. K. Mondal, and M. K. Gupta, "Developments and clinical evaluations of robotic exoskeleton technology for human upper-limb rehabilitation," *Advanced Robotics*, vol. 34, no. 15, pp. 1023–1040, 2020, doi: 10.1080/01691864.2020.1749926.

[43] D. Laparidou, F. Curtis, J. Akanuwe, K. Goher, A. Niroshan Siriwardena, and A. Kucukyilmaz, "Patient, carer, and staff perceptions of robotics in motor rehabilitation: a systematic review and qualitative meta-synthesis," *Journal of NeuroEngineering and Rehabilitation*, vol. 18, no. 1, 2021, doi: 10.1186/s12984-021-00976-3.

[44] G. A. Albanese *et al*., "Robotic systems for upper-limb rehabilitation in multiple sclerosis: a swot analysis and the synergies with virtual and augmented environments," *Frontiers in Robotics and AI*, vol. 11, 2024, doi: 10.3389/frobt.2024.1335147.

[45] F. Romero-Sánchez, L. Luporini Menegaldo, J. M. Font-Llagunes, and M. Sartori, "Rehabilitation robotics: Challenges in design, control, and real applications," *Frontiers in neurorobotics*, vol. 16, 2022, doi: 10.3389/978-2-88976-881-3.

[46] C. G. Rose, A. D. Deshpande, J. Carducci, and J. D. Brown, "The road forward for upper-extremity rehabilitation robotics," *Current Opinion in Biomedical Engineering*, vol. 19, 2021, doi: 10.1016/J.COBME.2021.100291.

[47] A. Akbari, F. Haghverd, and S. Behbahani, "Robotic home-based rehabilitation systems design: From a literature review to a conceptual framework for community-based remote therapy during covid-19 pandemic," *Frontiers in Robotics and AI*, vol. 8, 2021, doi: 10.3389/frobt.2021.612331.

[48] F. van Dellen and R. Labruyère, "Settings matter: a scoping review on parameters in robot-assisted gait therapy identifies the importance of

reporting standards," *Journal of NeuroEngineering and Rehabilitation*, vol. 19, no. 1, 2022, doi: 10.1186/s12984-022-01017-3.

[49] A. Garcia-Gonzalez, R. Q. Fuentes-Aguilar, I. Salgado, and I. Chairez, "A review on the application of autonomous and intelligent robotic devices in medical rehabilitation," *Journal of the Brazilian Society of Mechanical Sciences and Engineering*, vol. 44, no. 9, 2022, doi: 10.1007/s40430-022-03692-8.

[50] A. D. Banyai and C. Brișan, "Robotics in physical rehabilitation: Systematic review," *Healthcare*, vol. 12, no. 17, 2024, doi: 10.3390/healthcare12171720.

[51] Z. Z. Major *et al*., "The impact of robotic rehabilitation on the motor system in neurological diseases. a multimodal neurophysiological approach," *International Journal of Environmental Research and Public Health*, vol. 17, no. 18, 2020, doi: 10.3390/ijerph17186557.

[52] M. Maaref, A. Rezazadeh, K. Shamaei, and M. Tavakoli, "A gaussian mixture framework for co-operative rehabilitation therapy in assistive impedance-based tasks," *IEEE Journal of Selected Topics in Signal Processing*, vol. 10, no. 5, pp. 904–913, 2016, doi: 10.1109/JSTSP.2016.2532847.

[53] Y. Meng, C. Munroe, Y.-N. Wu, and M. Begum, "A learning from demonstration framework to promote home-based neuromotor rehabilitation," pp. 1126–1131, 2016, doi: 10.1109/ROMAN.2016.7745249.

[54] C. Martinez and M. Tavakoli, "Learning and reproduction of therapist's semi-periodic motions during robotic rehabilitation," *Robotica*, vol. 38, no. 2, pp. 337–349, 2019, doi: 10.1017/S0263574719000651.

[55] M. Sharifi, A. Zakerimanesh, J. K. Mehr, A. Torabi, V. K. Mushahwar, and M. Tavakoli, "Impedance variation and learning strategies in human–robot interaction," *IEEE Transactions on Cybernetics*, vol. 52, no. 7, pp. 6462–6475, 2022, doi: 10.1109/TCYB.2020.3043798.

[56] R. J. Escarabajal, J. L. Pulloquinga, P. Zamora-Ortiz, Á. Valera, V. Mata, and M. Vallés, "Imitation learning-based system for the execution of self-paced robotic-assisted passive rehabilitation exercises," *IEEE Robotics and Automation Letters*, vol. 8, no. 7, pp. 4283–4290, 2023, doi: 10.1109/LRA.2023.3281884.

[57] M. Maaref, A. Rezazadeh, K. Shamaei, R. Ocampo, and T. Mahdi, "A bicycle cranking model for assist-as-needed robotic rehabilitation therapy using learning from demonstration," *IEEE Robotics and Automation Letters*, vol. 1, no. 2, pp. 653–660, 2016, doi: 10.1109/LRA.2016.2525827.

[58] S. Pareek and T. Kesavadas, "iART: Learning From Demonstration for Assisted Robotic Therapy Using LSTM," in *IEEE Robotics and Automation Letters*, vol. 5, no. 2, pp. 477-484, 2020, doi: 10.1109/LRA.2019.2961845.

[59] S. F. Atashzar, M. Shahbazi, M. Tavakoli, and R. V. Patel, "A computational-model-based study of supervised haptics-enabled therapist-in-the-loop training for upper-limb poststroke robotic rehabilitation," *IEEE/ASME Transactions on Mechatronics*, vol. 23, no. 2, pp. 563–574, 2018, doi: 10.1109/TMECH.2018.2806918.

[60] M. Saveriano, F. J. Abu-Dakka, A. Kramberger, and L. Peternel, "Dynamic movement primitives in robotics: A tutorial survey," *The International Journal of Robotics Research*, vol. 42, no. 13, pp. 1133–1184, 2023, doi: 10.1177/02783649231201196.

[61] L.-H. Kong, W. He, W.-S. Chen, H. Zhang, and Y.-N. Wang, "Dynamic movement primitives based robot skills learning," *Machine Intelligence Research*, vol. 20, no. 3, pp. 396–407, 2023, doi: 10.1007/s11633-022-1346-z.

[62] Z. Lu, N. Wang and C. Yang, "A Dynamic Movement Primitives-Based Tool Use Skill Learning and Transfer Framework for Robot Manipulation," in *IEEE Transactions on Automation Science and Engineering*, 2024, doi: 10.1109/TASE.2024.3370139.

[63] I. Seleem, H. El-Hussieny and S. Assal, "Development of a Demonstration-Guided Motion Planning for Multi-section Continuum Robots," *2018 IEEE International Conference on Systems, Man, and Cybernetics (SMC)*, pp. 333-338, 2018, doi: 10.1109/SMC.2018.00066.

[64] I. A. Seleem, H. El-Hussieny, and H. Ishii, "Imitation-based path planning and nonlinear model predictive control of a multi-section continuum robots," *Journal of Intelligent & Robotic Systems*, vol. 108, no. 1, 2023, doi: 10.1007/s10846-023-01811-8.

[65] I. A. Seleem, S. F. Assal, H. Ishii, and H. El-Hussieny, "Guided pose planning and tracking for multi-section continuum robots considering robot dynamics," *IEEE Access*, vol. 7, pp. 166690–166703, 2019, doi: 10.1109/ACCESS.2019.2953122.

[66] P. Pastor, H. Hoffmann, T. Asfour and S. Schaal, "Learning and generalization of motor skills by learning from demonstration," *2009 IEEE International Conference on Robotics and Automation*, pp. 763-768, 2009, doi: 10.1109/ROBOT.2009.5152385.

[67] C. Tamantini, M. Lapresa, F. Cordella, F. Scotto di Luzio, C. Lauretti, and L. Zollo, "Combined use of DMP and real objects in robot-aided rehabilitation," *2020 I-RIM Conference,* 2020, doi: 10.5281/zenodo.4781572.

[68] C. Lauretti, F. Cordella, E. Guglielmelli, and L. Zollo, "Learning by demonstration for planning activities of daily living in rehabilitation and assistive robotics," *IEEE Robotics and Automation Letters*, vol. 2, no. 3, pp. 1375–1382, 2017, doi: 10.1109/LRA.2017.2669369.

[69] A. J. Ijspeert, J. Nakanishi, H. Hoffmann, P. Pastor, and S. Schaal, "Dynamical movement primitives: Learning attractor models for motor behaviors," *Neural Computation*, vol. 25, no. 2, pp. 328–373, 2013, doi: 10.1162/NECO_a_00393.

[70] W. Kim, C. Lee, and H. J. Kim, "Learning and generalization of dynamic movement primitives by hierarchical deep reinforcement learning from demonstration," vol. 11, pp. 3117–3123, 2018, doi: 10.1109/IROS.2018.8594476.

[71] H. Ravichandar, A. S. Polydoros, S. Chernova, and A. Billard, "Recent advances in robot learning from demonstration," *Annual review of control, robotics, and autonomous systems*, vol. 3, no. 1, pp. 297–330, 2020, doi: 10.1146/annurev-control-100819-063206.

[72] W. Si, N. Wang, and C. Yang, "A review on manipulation skill acquisition through teleoperation-based learning from demonstration," *Cognitive Computation and Systems*, vol. 3, no. 1, pp. 1–16, 2021, doi: 10.1049/ccs2.12005.

[73] S. Hu, R. Mendonca, M. J. Johnson, and K. J. Kuchenbecker, "Robotics for occupational therapy: Learning upper-limb exercises from demonstrations," *IEEE Robotics and Automation Letters*, vol. 6, no. 4, pp. 7781–7788, 2021, doi: 10.1109/LRA.2021.3098945.

[74] D. A. Duque, F. A. Prieto, and J. G. Hoyos, "Trajectory generation for robotic assembly operations using learning by demonstration," *Robotics and Computer-Integrated Manufacturing*, vol. 57, pp. 292–302, 2019, doi: 10.1016/j.rcim.2018.12.007.

[75] A. D. Sosa-Ceron, H. G. Gonzalez-Hernandez, and J. A. Reyes-Avendaño, "Learning from demonstrations in human–robot collaborative scenarios: A survey," *Robotics*, vol. 11, no. 6, 2022, doi: 10.3390/robotics11060126.

[76] Z. Lu, N. Wang, and C. Yang, "A constrained dmps framework for robot skills learning and generalization from human demonstrations," *IEEE/ASME Transactions on Mechatronics*, vol. 26, no. 6, pp. 3265–3275, 2021, doi: 10.1109/TMECH.2021.3057022.

[77] J. Li, Z. Li, X. Li, Y. Feng, Y. Hu, and B. Xu, "Skill learning strategy based on dynamic motion primitives for human–robot cooperative manipulation," *IEEE Transactions on Cognitive and Developmental Systems*, vol. 13, no. 1, pp. 105–117, 2021, doi: 10.1109/TCDS.2020.3021762.

[78] J. Li, M. Cong, D. Liu, and Y. Du, "Enhanced task parameterized dynamic movement primitives by gmm to solve manipulation tasks," *Robotic Intelligence and Automation*, vol. 43, no. 2, pp. 85–95, 2023, doi: 10.1108/ria-07-2022-0199.

[79] Y. Wang, W. Li, and Y. Liang, "A trajectory optimisation-based incremental learning strategy for learning from demonstration," *Applied Sciences*, vol. 14, no. 11, 2024, doi: 10.3390/app14114943.

[80] Z. Lu, N. Wang, and D. Shi, "Dmps-based skill learning for redundant dual-arm robotic synchronized cooperative manipulation," *Complex & Intelligent Systems*, vol. 8, no. 4, pp. 2873–2882, 2021, doi: 10.1007/s40747-021-00429-3.

[81] A. Li, Z. Liu, W. Wang, M. Zhu, Y. Li, Q. Huo, and M. Dai, "Reinforcement learning with dynamic movement primitives for obstacle avoidance," *Applied Sciences*, vol. 11, no. 23, 2021, doi: 10.3390/app112311184.

[82] G. Li, Z. Jin, M. Volpp, F. Otto, R. Lioutikov, and G. Neumann, "Prodmp: A unified perspective on dynamic and probabilistic movement primitives," *IEEE Robotics and Automation Letters*, vol. 8, no. 4, pp. 2325–2332, 2023, doi: 10.1109/LRA.2023.3248443.

[83] S. Shaw, D. K. Jha, A. Raghunathan, R. Corcodel, D. Romeres, G. Konidaris, and D. Nikovski, "Constrained dynamic movement primitives for safe learning of motor skills," *arXiv* 2022, doi: 10.48550/arXiv.2209.14461.

[84] M. Ginesi, N. Sansonetto, and P. Fiorini, "Overcoming some drawbacks

of dynamic movement primitives," *Robotics and Autonomous Systems*, vol. 144, 2021, doi: 10.1016/j.robot.2021.103844.

[85] S. Qiu, W. Guo, D. Caldwell, and F. Chen, "Exoskeleton online learning and estimation of human walking intention based on dynamical movement primitives," *IEEE Transactions on Cognitive and Developmental Systems*, vol. 13, no. 1, pp. 67–79, 2021, doi: 10.1109/TCDS.2020.2968845.

[86] A. S. Anand, A. Østvik, E. I. Grøtli, M. Vagia and J. T. Gravdahl, "Real-time temporal adaptation of dynamic movement primitives for moving targets," *2021 20th International Conference on Advanced Robotics (ICAR)*, pp. 261-268, 2021, doi: 10.1109/ICAR53236.2021.9659384.

[87] F. A. Zaini, M. F. Sulaima, I. A. W. A. Razak, N. I. Zulkafli, and H. Mokhlis, "A review on the applications of pso-based algorithm in demand side management: challenges and opportunities," *IEEE Access*, vol. 11, pp. 53373–53400, 2023, doi: 10.1109/access.2023.3278261.

[88] J. Cai, H. Wei, H. Yang, and X. Zhao, "A novel clustering algorithm based on dpc and pso," *IEEE Access*, vol. 8, p. 88200–88214, 2020, doi: 10.1109/access.2020.2992903.

[89] M. Jain, V. Saihjpal, N. Singh, and S. B. Singh, "An overview of variants and advancements of pso algorithm," *Applied Sciences*, vol. 12, no. 17, 2022, doi: 10.3390/app12178392.

[90] H. Moayedi, M. Mehrabi, M. Mosallanezhad, A. S. A. Rashid, and B. Pradhan, "Modification of landslide susceptibility mapping using optimized pso-ann technique," *Engineering with Computers*, vol. 35, no. 3, p. 967–984, 2018, doi: 10.1007/s00366-018-0644-0.

[91] A. Tharwat and W. Schenck, "A conceptual and practical comparison of pso-style optimization algorithms," *Expert Systems with Applications*, vol. 167, 2021, doi: 10.1016/j.eswa.2020.114430.

[92] L. Sciavicco and B. Siciliano, "Modelling and control of robot manipulators," *Measurement Science and Technology*, vol. 11, no. 12, 2000, doi: 10.1088/0957-0233/11/12/709.

[93] D. E. Whitney, "Resolved motion rate control of manipulators and human prostheses," *IEEE Transactions on Man-Machine Systems*, vol. 10, no. 2, pp. 47–53, 1969, doi: 10.1109/TMMS.1969.299896.

[94] B. Zhou, L. Yang, C. Wang, Y. Chen, and K. Chen, "Inverse jacobian adaptive tracking control of robot manipulators with kinematic, dynamic, and actuator uncertainties," *Complexity*, vol. 2020, no. 1, 2020, doi: 10.1155/2020/5070354.

[95] P. Chiacchio and B. Siciliano, "A closed-loop jacobian transpose scheme for solving the inverse kinematics of nonredundant and redundant wrists," *Journal of Robotic Systems*, vol. 6, no. 5, pp. 601–630, 1989, doi: 10.1002/rob.4620060507.

[96] C. M. Martinez, J. Fong, S. F. Atashzar, and M. Tavakoli, "Semi-autonomous robot-assisted cooperative therapy exercises for a therapist's interaction with a patient," in *2019 IEEE Global Conference on Signal and Information Processing (GlobalSIP)*, 2019, pp. 1–5, doi: 10.1109/GlobalSIP45357.2019.8969143.

[97] M. Najafi, K. Adams, and M. Tavakoli, "Robotic learning from demonstration of therapist's time-varying assistance to a patient in trajectory-following tasks," in *2017 International Conference on Rehabilitation Robotics (ICORR)*, 2017, pp. 888–894, doi: 10.1109/ICORR.2017.8009361.